

Prediction Errors and Local Lyapunov Exponents

Matthew B. Kennel*

Institute for Nonlinear Science

and

Department of Physics

Henry D. I. Abarbanel†

Department of Physics

and

Marine Physical Laboratory

Scripps Institution of Oceanography

and

Institute for Nonlinear Science

J. J. (“Sid”) Sidorowich‡

Institute for Nonlinear Science University of California, San Diego

Mail Code 0402

La Jolla, CA 92093-0402

(November 7, 2018)

Abstract

It is frequently asserted that in a chaotic system two initially close points will separate at an exponential rate governed by the largest global Lyapunov exponent. Local Lyapunov exponents, however, are more directly relevant to predictability. The difference between the local and global Lyapunov exponents, the large variations of local exponents over an attractor, and the saturation of error growth near the size of the attractor—all result in non-exponential scalings in errors at both short and long prediction times, sometimes even obscuring evidence of exponential growth. Failure to observe exponential error scaling cannot rule out deterministic chaos as an explanation. We demonstrate a simple model that quantitatively predicts observed error scaling from the local Lyapunov exponents, for both short and surprisingly long times. We comment on the relevance to atmospheric predictability as studied in the meteorological literature.

05.45.+b,92.60.Wc

Typeset using REVTeX

Chaotic behavior in dynamical systems is intermediate between precisely predictable, regular evolution and completely unpredictable, stochastic evolution. The global Lyapunov exponents [1,2] quantify the evolution of perturbations as the system evolves for long times. A positive global Lyapunov exponent implies that errors grow to the overall size of the attractor limiting predictability to finite times.

Given observed data from a chaotic source, one can construct accurate empirical predictors [3,4,6] which allow predictions for finite times—without any knowledge of the underlying dynamics. Positive global Lyapunov exponents causes the errors in these predictions to grow exponentially rapidly, and it is conventionally assumed that the prediction error $E(t)$ will grow as

$$E(t) = E(0) \exp(\lambda_1 t). \quad (1)$$

λ_1 is the largest global Lyapunov exponent. Indeed this error growth is used as a diagnostic of deterministic chaos in the analysis of observed data [4,5].

This paper is devoted to a closer examination of this common assumption, and we will show it is often *incorrect* for times where the system is predictable. For $t \rightarrow \infty$ the largest global Lyapunov exponent λ_1 is defined in terms of a long-term average growth rate, but it does not always reflect the actual growth of prediction errors in finite time. Further for $t \rightarrow \infty$ the perturbed orbit, although eventually uncorrelated with the reference orbit, is constrained to stay on the attractor, and thus the size of a perturbation will saturate near the overall size of the attractor. Reconciling these two aspects of error growth leads to our improvement to Equation (1).

We briefly review the definition of local Lyapunov exponents. Our discrete time dynamical system is $\mathbf{y}(n+1) = \mathbf{F}(\mathbf{y}(n))$. Small perturbations $\delta\mathbf{y}(n)$ to this orbit evolve L steps forward in time according to the linearized dynamics

$$\delta\mathbf{y}(n+L) = \mathbf{DF}^L(\mathbf{y}(n)) \cdot \delta\mathbf{y}(n). \quad (2)$$

With $\mathbf{DF}_{ab}(\mathbf{y}) = \partial F_a(\mathbf{y}) / \partial y_b$ the Jacobian matrix of the dynamics, we denote $\mathbf{DF}^L(\mathbf{y}(n)) = \prod_{i=0}^{L-1} \mathbf{DF}(\mathbf{y}(n+i))$. The Oseledec matrix [2],

$$\mathbf{O}(\mathbf{y}, L) = \left[(\mathbf{DF}^L(\mathbf{y}))^T \cdot \mathbf{DF}^L(\mathbf{y}) \right]^{1/2L} \quad (3)$$

has eigenvalues $e^{\lambda_1(\mathbf{y},L)}, e^{\lambda_2(\mathbf{y},L)}, \dots, e^{\lambda_d(\mathbf{y},L)}$, in d -dimensions. We order the exponents as $\lambda_1 \geq \lambda_2 \geq \lambda_3 \dots \geq \lambda_d$. These **local** exponents $\lambda_a(\mathbf{y}, L)$ address the growth (or decay) over L time steps of perturbations made around some point \mathbf{y} in the state space. As $L \rightarrow \infty$ $\lambda_a(\mathbf{y}, L) \rightarrow \lambda_a$, the global exponents.

Taken over an initially isotropic distribution the initial root-mean-squared Euclidean distance of the *evolved* perturbation vectors to the origin will grow by $(\frac{1}{d} \sum_{i=1}^d \Lambda_i^2)^{1/2}$. $\Lambda_a(\mathbf{x}, L) = \exp[L\lambda_a(\mathbf{x}, L)]$. Lorenz first derived this formula in an early paper [9]. We employ the analogous quantity appropriate for a geometric mean instead of the arithmetic mean. We found this to be $\frac{1}{d} \sum_{i=1}^d \Lambda_i$ via numerical experiment, though we do not yet know of a simple, general derivation corresponding to that in reference [9]. We note that direct numerical computation of the matrix product of many Jacobians leads to ill-conditioning, and thus for practical computation we employ the algorithm of reference [8] to stably compute the local Lyapunov exponents.

The quantity $E(\mathbf{x}, L) = \frac{1}{d} \sum_{i=1}^d \Lambda_i(\mathbf{x}, L)$, which we denote the “expansion factor”, quantifies the multiplicative growth of typical predictor errors starting at \mathbf{x} , looking ahead L steps. The expansion factor is best calculated from local exponents as

$$\begin{aligned} \log E(\mathbf{x}, L) = & L\lambda_1(\mathbf{x}, L) + \log[1 + e^{L(\lambda_2(\mathbf{x},L)-\lambda_1(\mathbf{x},L))} + e^{L(\lambda_3(\mathbf{x},L)-\lambda_1(\mathbf{x},L))} + \dots \\ & + e^{L(\lambda_d(\mathbf{x},L)-\lambda_1(\mathbf{x},L))}] - \log d \end{aligned} \quad (4)$$

For increasing L , $\lambda_1(\mathbf{x}, L)$ quickly dominates the expansion factor. This also motivates Equation (1), but here $\lambda_1(\mathbf{x}, L)$, is the *finite-time* Lyapunov exponent, which does not converge very quickly to λ_1 . [7].

The other ingredient in our model for the average prediction error is a saturation cutoff. If we limit the maximal expansion factor for each initial condition to a constant R , we then compute the geometric mean (over reference points on the attractor $\mathbf{x}(i)$) of the expansion factors $E(\mathbf{x}, L)$, which is the arithmetic mean of $\log E(\mathbf{x}, L)$, hard-limited by $\rho = \log R$:

$$\log X(L, \rho) = \frac{1}{N} \sum_{i=1}^N \min [\log E(\mathbf{x}(i), L), \rho] - \rho. \quad (5)$$

The saturation cutoff models the fact that finite-sized perturbations and prediction errors cannot grow indefinitely. We estimate R is the ratio of the geometric mean of $|\mathbf{x}(i) - \mathbf{x}(j)|$ over uncorrelated pairs of attractor points to the geometric mean of the initial perturbation

magnitude. Larger R corresponds to better predictability. Note that we are averaging individually thresholded expansion factors—not thresholding an average expansion factor. Before the saturation sets in $\log X(L) \approx L\bar{\lambda}(L)$, with $\bar{\lambda}(L)$ the average finite-time Lyapunov exponent [7,8].

We now compare (1) the growth of errors actually incurred by making repeated predictions and (2) the growth rate implied by the thresholded expansion factors, Equation (5). This suggests that prediction errors grow as do the separation of initially close trajectories. This means we are considering the errors in prediction that arise from inherent dynamical instability and not inaccuracies as a result of specific features of the prediction scheme.

Our measure of average prediction error is the geometric mean over initial conditions of an L -step iterated predictor, a composition of L one-step predictors. The error is normalized by the geometric mean distance between all time-decorrelated pairs of points on the attractor, so that the absence of predictability corresponds to zero logarithmic error. With $\mathbf{G}(\bullet)$ the one-step predictor, the normalized prediction error L steps ahead is

$$\log \chi(L) = \frac{1}{N} \sum_{i=1}^N \log |\mathbf{G}^L(\mathbf{x}(i)) - \mathbf{x}(i+L)| - \frac{1}{N^2} \sum_{i,j=1}^N \log |\mathbf{x}(i) - \mathbf{x}(j)|. \quad (6)$$

As for $\log X(L, \rho) \lim_{L \rightarrow \infty} \log \chi(L) = 0$. The iterated prediction is *not* rescaled to remain close to the reference trajectory.

The main empirical result is that on chaotic attractors $\log \chi(L) = \log X(L, \rho)$ given the correct threshold ρ . We evaluate the local Lyapunov exponents, then compute the single parameter family of curves given by Equation (5) over a range of ρ . We find that once the best value of ρ is found, the resulting $\log X(L, \rho)$ quantitatively predicts the scaling of errors throughout the range of time examined. That equation (5) predicts the scaling of errors in the saturation region ($L \rightarrow \infty$) is somewhat surprising because Lyapunov exponents quantify linear expansion rates of *infinitesimal* perturbations, but in the saturation region one envisions typically large deviations. A possible explanation is that in the saturation regime average prediction error is controlled by the tail of the distribution of individual expansion factors: those initial conditions that happen to be exceptionally predictable and whose expansion factors thus remain below the threshold for especially long times. This is plausible because local Lyapunov exponents often have wide distributions [7,8].

Figure 1 shows iterated prediction errors, $\log_{10}(\chi(L))$, computed using nonlinear kernel regression [6] versus thresholded expansion factors (5) for data from the Ikeda map of the

plane to itself [10]. The data set is 20,000 real and imaginary components from the complex-valued map $z(n+1) = p + Bz(n) \exp[i\kappa - i\alpha/(1 + |z(n)|^2)]$ with parameters $p = 1.0$, $B = 0.9$, $\kappa = 0.4$, $\alpha = 6.0$. At short times, there is an obvious exponential scaling region (a line with a constant slope λ_1), as predicted by Equation (1). Starting at $L \approx 10$ the slope decreases and curves off to zero, well modeled by the thresholded expansion factor. We did not optimize ρ in any sophisticated manner, but simply stepped ρ by 0.2 and selected the best match. From a time series $\mathbf{y}(i), i = 1 \dots N$, we compute a prediction for an input vector \mathbf{x} as $\mathbf{G}(\mathbf{x}) = \left(\sum_{i=1}^N \mathbf{y}(i+1) K(\mathbf{x} - \mathbf{y}(i)) \right) / \left(\sum_{i=1}^N K(\mathbf{x} - \mathbf{y}(i)) \right)$ using a Gaussian kernel $K(\mathbf{z}) = \exp(-|\mathbf{z}|^2/\sigma^2)$ with σ set to twice the geometric mean nearest-neighbor distance of the $\mathbf{y}(i)$. This is a global prediction formula but effectively functions as a localized interpolator. The local Lyapunov exponents were calculated from this same data set [8] without the equations.

Figure 2 shows the same information for data from a three dimensional flow of Lorenz [11]. The dynamical equations are $\dot{x} = -y^2 - z^2 - a(x - F)$, $\dot{y} = xy - bxz - y + G$, $\dot{z} = bxy + xz - z$, with parameters set $a = 0.25$, $b = 4.0$, $F = 8.0$, and $G = 1.0$, sampled at intervals $\delta t = 0.2$. The attractor has a dimension of about 2.5. There is no obvious exponential scaling regime here. Given only the curve of predictor errors, one could not easily identify the Lyapunov exponent, in contrast to the previous example. The appropriately thresholded expansion factor, however, agrees with the observed scaling of prediction errors. For contrast, the graph also shows the results of choosing either too small a threshold (the circles) or too large a threshold (the triangles) for this prediction scheme and data set.

Now we examine our main result $\log \chi(L) = \log X(L, \rho)$ with a better controlled experiment. This time as our “prediction function” we use the actual dynamical equations of the Lorenz system but start the integration with an initial condition slightly perturbed from the reference point by a small uniformly distributed random vector $\eta(i)$: $\mathbf{G}^L(\mathbf{x}(i)) = \mathbf{F}^L(\mathbf{x}(i) + \eta(i))$. We directly calculate Lyapunov exponents from the known differential equations by simultaneously integrating the equations of motion and the tangent space flow. Figure 3 compares $\log \chi(L)$ with $\log X(L, \rho)$ with varying sizes of the initial perturbation. The growth of the perturbations matches the thresholded expansion factor, with the previously free parameter ρ fixed at the predicted value $\rho = \langle \log |\mathbf{x}(i) - \mathbf{x}(j)| \rangle_{i,j=1 \dots N} - \langle \log |\eta(i)| \rangle_{i=1 \dots N}$, confirming our model.

This scaling with L is generic to most low dimensional flows: a curve at low L scaling with an initially high slope, because the average largest local exponent is larger than the global

exponent [8], an exponential region (constant slope) corresponding to the global Lyapunov exponent, and a long tail curving off to zero as the finite-size threshold takes effect. The size and existence of the region of constant slope depends on the size of the initial error. If the error is large enough, there may be no region of exponential scaling as the curvature due to finite-time exponents merges with the curvature due to thresholds. Higher-dimensional data are likely to have lower initial predictability than very low-dimensional attractors, and therefore likely to show little observably exponential error scaling. Intermittent dynamics will create a wide variation in finite-time Lyapunov exponents, thus moving forward the time where saturation begins to take effect. In analyzing dynamical systems more complex than simple one or two dimensional models, requiring manifestly exponential error scaling as confirming deterministic chaos is unrealistic.

We have identified empirical prediction error with the evolution of perturbations, but the identity does not always strictly hold. Figure 4 shows the prediction errors on the same Lorenz flow [11] data using an accurate local quadratic polynomial technique [4,5]. This time, the prediction error is not satisfactorily matched by the thresholded expansion factor with any ρ , the main difference being a substantially larger slope at small L . We attribute part of this discrepancy to the assumption, used in deriving the expansion factor, that the initial perturbations are distributed uniformly in all directions. When a very accurate model, such as this one, is combined with extremely clean data, short term forecasting errors will be quite small, and the predicted trajectory will closely shadow the attractor, and thus, the unstable manifold. Therefore the initial rate of expansion will be larger than for isotropically distributed errors, being described better by a new “primary” expansion factor $L\lambda_1(\mathbf{x}, L)$ that only considers error expansion due to the single *largest* local Lyapunov exponent. This quantity increases faster at short times than the standard expansion factor, but still, it fails to precisely match the scaling of forecast error. Another discrepancy not accounted for by the expansion factor is that iterating imperfect models injects new error at every timestep, not only at the beginning. Usually exponential expansion of old error dominates new error, except at the shortest times. This effect will cause yet another increase to the slope at small times. When we add some isotropic noise to the initial condition before applying the iterated local predictor, outstanding agreement with the scaling predicted by Equation (5) is restored. We note that the divergence between straight prediction error and expansion factor is exaggerated by the particular conditions in force here: very good prediction on a

data base of very clean low-dimensional data from a smooth chaotic flow. We performed the same test on noisier experimental chaotic data and saw a smaller difference.

Is adding noise to the initial condition “cheating”? To be completely rigorous, one ought to model the distribution of prediction errors in the various directions corresponding to the local Lyapunov exponents. This is not possible without knowledge of detailed properties of the specific prediction scheme, and is obviously beyond the scope of this paper. The approximation of isotropic perturbation may often be acceptable, and can be enforced by adding artificial noise. In the context of analyzing observed data, a successful match between prediction errors (even with artificial initial perturbations) and thresholded expansion factors is a novel cross-check that affirms the validity of the modeling procedures, even if one cannot exactly quantify the error scaling for a particular prediction scheme. Accurate evaluation of Lyapunov exponents from degraded or high-dimensional data is somewhat difficult in practice, requiring good estimates of derivatives of the implied evolution function. Various reconstruction parameters, such as embedding and local manifold dimensions and time delay [8,3] may yield substantially different numerical answers for Lyapunov exponents, even if all are topologically acceptable. Further requiring a good match between expansion factors and error scaling provides a criterion for selecting among the otherwise equivalent choices. In general, we have found that prediction error scaling varies less with reconstruction parameters than Lyapunov exponents.

Figure 5 shows $\langle \log E(\mathbf{x}(i), L) \rangle$ ($\log X$ without the threshold) for the Lorenz flow. At the smallest times, the expansion factor does not in fact possess a constant slope, and only flattens out to a straight line, with slope equal to the infinite-time Lyapunov exponent after an initial transient regime. This curvature is always in the direction seen on this graph (higher slope at shorter times) and is a result of the fact that the average local Lyapunov exponent $\bar{\lambda}(L)$ approaches the global exponent from above as $L \rightarrow \infty$ [8]. This curvature explains non-exponential scaling of prediction error for early time intervals. Also shown is the mean plus and minus one standard deviation of the distribution of individual expansion factors $E(\mathbf{x}, L)$. The Figure demonstrates that the variation in local exponents as a function of initial condition causes a wide variation in expansion factor that *increases* with increasing L . The interaction of this wide distribution with the threshold results in the saturation of prediction error for longer times. The effects of the finite size of the attractor begin to manifest themselves when an appreciable number of the individual expansion factors approach the cutoff, which occurs well before the mean expansion factor does so.

Notice that the width of the distribution *increases* as $L \rightarrow \infty$; we have observed this feature in all systems we examined. An important conclusion is that even though the local Lyapunov exponent converges to a single global exponent which is *independent of initial condition*, i.e. $\lim_{L \rightarrow \infty} \lambda_1(\mathbf{x}, L) = \lambda_1$, the expansion factors of various individual initial conditions do not do so: $\lim_{L \rightarrow \infty} E(\mathbf{x}, L) \neq \bar{E}(L)$. This is because the standard deviation of the distribution of local exponents $\langle (\lambda(\mathbf{x}, L) - \bar{\lambda}(L))^2 \rangle$ typically decreases at a rate substantially slower than L^{-1} . Of course, considering global saturation, normalized error will eventually converge to unity, but this is an entirely different mechanism. The message is that considering dynamical predictability solely in view of the largest global Lyapunov exponent may be conceptually misleading as well as quantitatively inaccurate.

The temporal development of forecast error has been a prime concern of the weather forecasting community for many years, starting with work of Lorenz [9,12]. Common practice has been to hypothesize *ad hoc* relationships for the average error as a function of time; usually, in the form of a differential equation. Lorenz found [12] that increase of mean deviation between initially close initial atmospheric states could be fitted by an empirical law of the form

$$\dot{E}(t) = \alpha E(t) (1 - E(t)/E(\infty)). \quad (7)$$

A positive Lyapunov exponent motivates the first term; the inevitable saturation at maximum error, the second. Stroe and Royer [13] compared generalized parameterizations of empirical growth laws that include Lorenz's with results of large-scale atmospheric simulations and some experimental observations. The scaling of mean error at larger times, in the saturation regime, appeared to be better fit by an exponential law such as $d \log E(t)/dt = -\beta \log E(t)$, similar to results seen in our work, but a single empirical rule governing the initial growth of errors was not clearly indicated, either in this or previous studies. We explain this with the fact that the initial growth of error is governed by finite-time, rather than global, Lyapunov exponents. This results in an initial regime of non-exponential growth, second, this error growth rate depends on the coordinate system used [7]. The differing measures of phase-space distance employed by atmospheric scientists will result in different growth rates making the notion of a universal "doubling time for small errors" less useful than commonly believed. Our modeling of the error growth, which holds the mean finite-time Lyapunov exponents responsible at small error, but with their variation most important at saturation, backs up Stroe and Royer's conclusions that the infinitesimal

growth rate cannot be easily deduced from the saturation rate via fitting a single empirical formula like equation (7). One further point that we wish to make is that we have observed that using the arithmetic mean for the ensemble average of both error and expansion factors rather than the geometric results in far more “noisy” curves, and thus is it not clear whether expansion factors accurately match prediction errors with ensemble averaging in the arithmetic sense, though we suspect so. The arithmetic mean, commonly employed in meteorological literature, seems to be dominated by fluctuations in a few samples in the large error tail of the distribution. Convergence of the arithmetical ensemble average appears to require numbers of points excessively large even for this low-dimensional investigation. Choosing an arithmetical average also appears to accentuate the initial superexponential growth. Still, the qualitative behavior of error scaling seen in large-scale atmospheric simulations and experiment [13] appears compatible with our model, which we suggest as a more fundamental explanation for observed error growth. In the nonlinear dynamics literature, one example in Farmer and Sidorowich [4] demonstrated initially faster-than-exponential error scaling, but remained unexplained in that work.

With the exception of the work of Lorenz [9], the direct use of local Lyapunov exponents to quantify error growth in atmospheric dynamics is rather recent [14–16] and remains open to further development. The Lyapunov exponents have generally been previously considered only in the context of infinitesimal errors. This present work shows that accounting for a threshold apparently allows finite-time Lyapunov exponents to quantify error scaling at both small and substantially larger levels of error. Work remains concerning more realistic models, of course. Results of other low-dimensional chaotic data sets that we have examined, including experimental data, agree with the conclusions of this paper.

REFERENCES

* E-mail: mbk@inls1.ucsd.edu

† E-mail: hdia@hamilton.ucsd.edu

‡ E-mail: sid@inls1.ucsd.edu

- [1] Eckmann, J.-P. and D. Ruelle “Ergodic Theory of Chaos and Strange Attractors” *Rev. Mod. Phys.* **57**, 617 (1985).
- [2] Oseledec, V. I., “A Multiplicative Ergodic Theorem. Lyapunov Characteristic Numbers for Dynamical Systems” *Trudy Mosk. Mat. Obsc* **19**, 197 (1968); *Moscow Math. Soc.* **19**, 197 (1968).
- [3] Abarbanel, H. D. I., R. Brown, J. (“Sid”) Sidorowich, and Lev Sh. Tsimring, “The Analysis of Observed Chaotic Data in Physical Systems”, *Reviews of Modern Physics* **65**, 1331-1392 (1993).
- [4] J. D. Farmer and J. Sidorowich, *Phys. Rev. Lett.*, **59**, 845 (1987)
- [5] J. D. Farmer and J. Sidorowich, “Exploiting Chaos to Predict the Future and Reduce Noise”. In *Evolution, Learning and Cognition*, ed. Y.C. Lee, World Scientific, Singapore (1988)
- [6] H. D. I. Abarbanel, R. Brown, and J. B. Kadtko, “Prediction in Chaotic Nonlinear Systems: Methods for Time Series with Broadband Fourier Spectra”, *Phys. Rev. A* **41**, 1782 (1990).
- [7] H. D. I. Abarbanel, R. Brown, and M. B. Kennel , “Variability of Lyapunov Exponents on a Strange Attractor”, *Journal of Nonlinear Science*, **1**, 175-199 (1991).
- [8] H. D. I. Abarbanel, R. Brown, and M. B. Kennel, “Local Lyapunov Exponents from Observed Data”, *Journal of Nonlinear Science* **2**, 343-365 (1992).
- [9] E. N. Lorenz, *Tellus* **17**, 321–333 (1965)
- [10] K. Ikeda, *Opt. Commun.* **30**, 257 (1979).
- [11] E. N. Lorenz, *Tellus* **36A**, 98-110 (1984).
- [12] E. N. Lorenz, *J. Atmos. Sci.* **26** 636–646 (1969)
- [13] R. Stroe, J.F. Royer, *Ann. Geophysicae* **11**, 296–316 (1993)
- [14] B.F. Farrell *J. Atmos. Sci.* **47** 2409–2416 (1990)
- [15] J.M. Nese, J.A. Dutton *J. Climate* **6** 185–203 (1993)
- [16] S. Yoden, M. Nomura *J. Atmos. Sci* **50** 1531–1543 (1993)

FIGURES

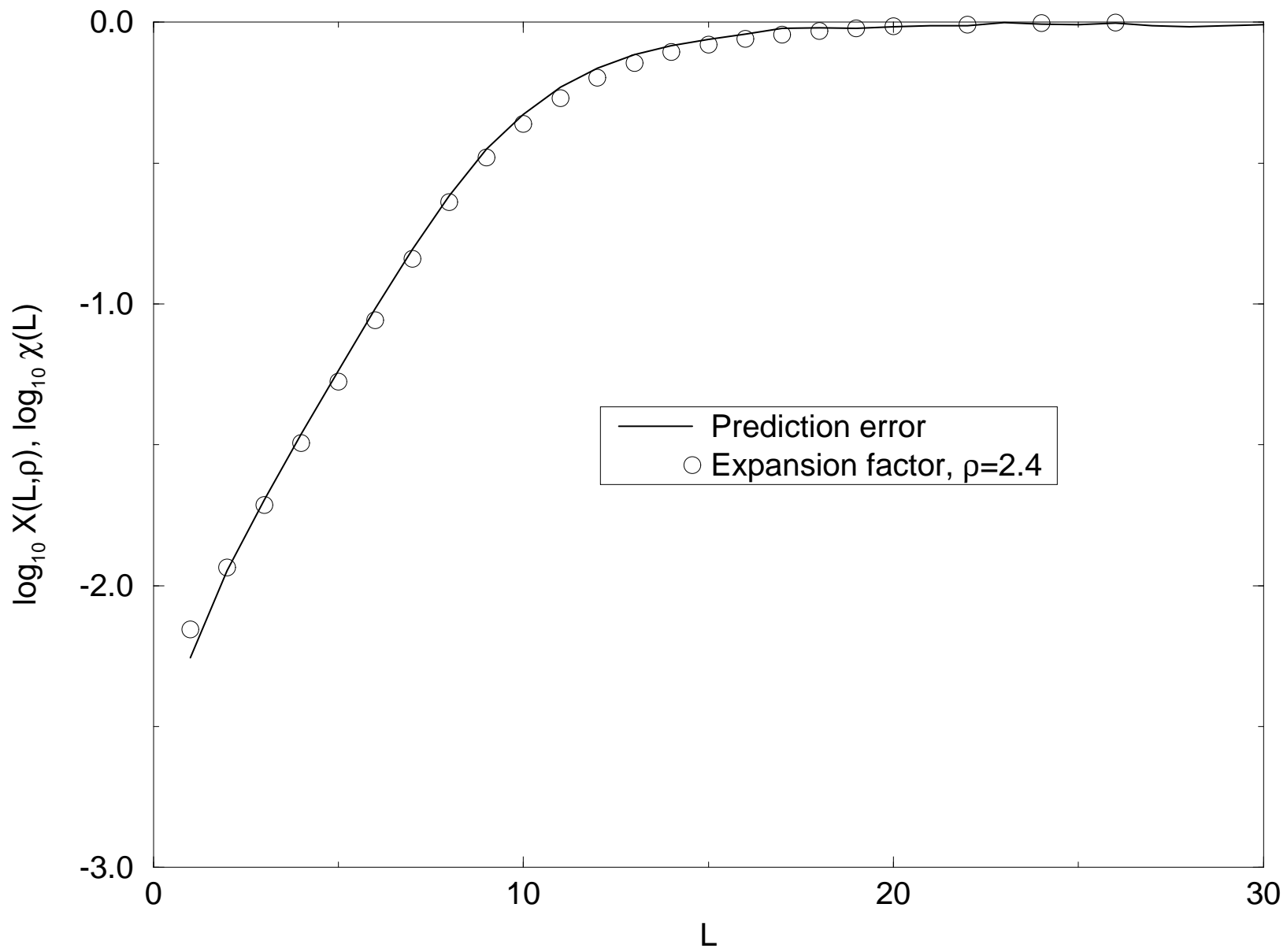
FIG. 1. $\log_{10} \chi(L)$ (solid line) and $\log_{10} X(L, \rho)$ (circles) for the Ikeda map. $\rho = 2.4$ gives a good fit.

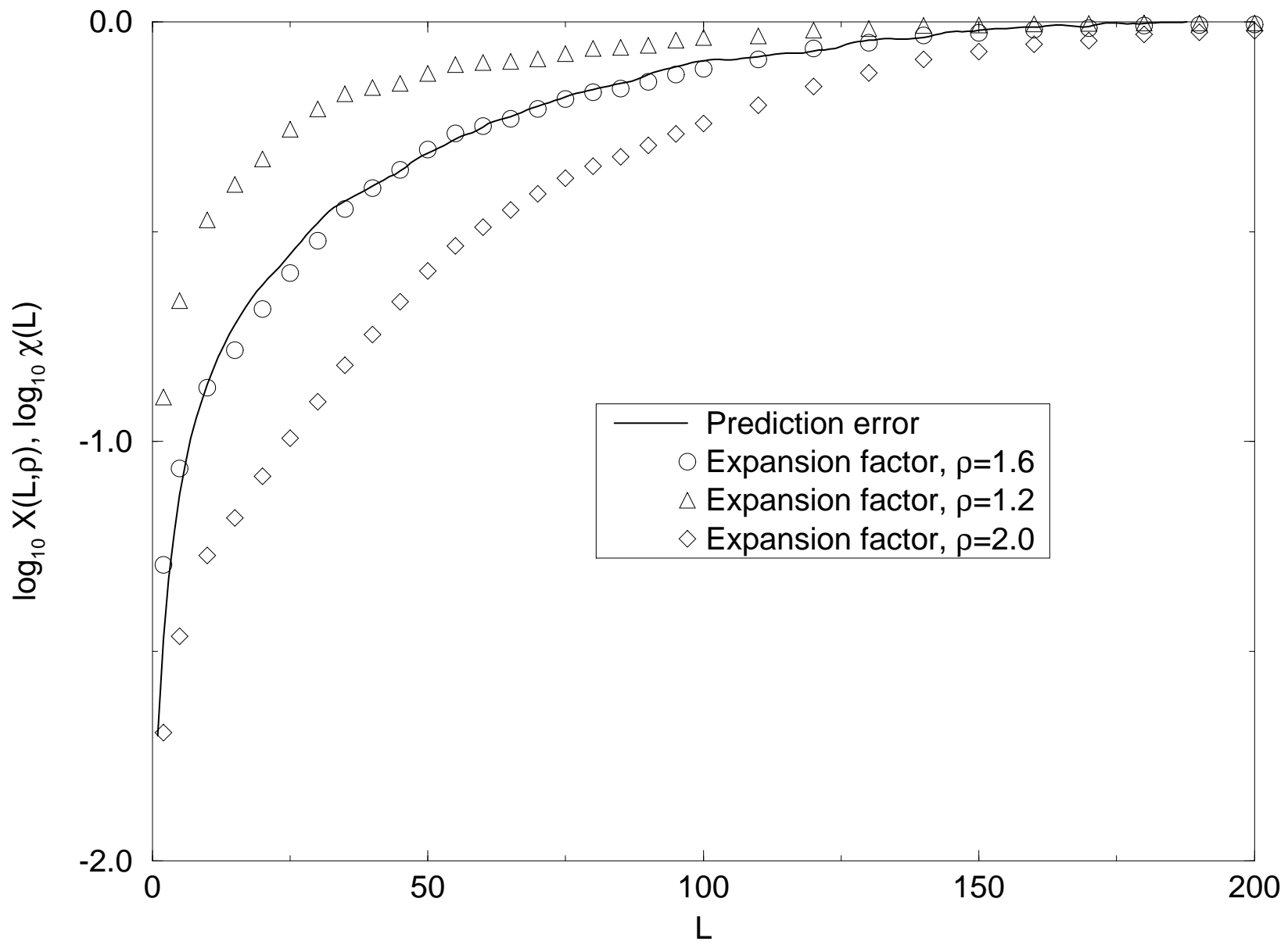
FIG. 2. $\log_{10} \chi(L)$ (solid line) and $\log_{10} X(L, \rho)$ for data from the Lorenz flow, with $\rho = 1.2$ (triangles), $\rho = 1.6$ (circles), and $\rho = 2.0$ (diamonds).

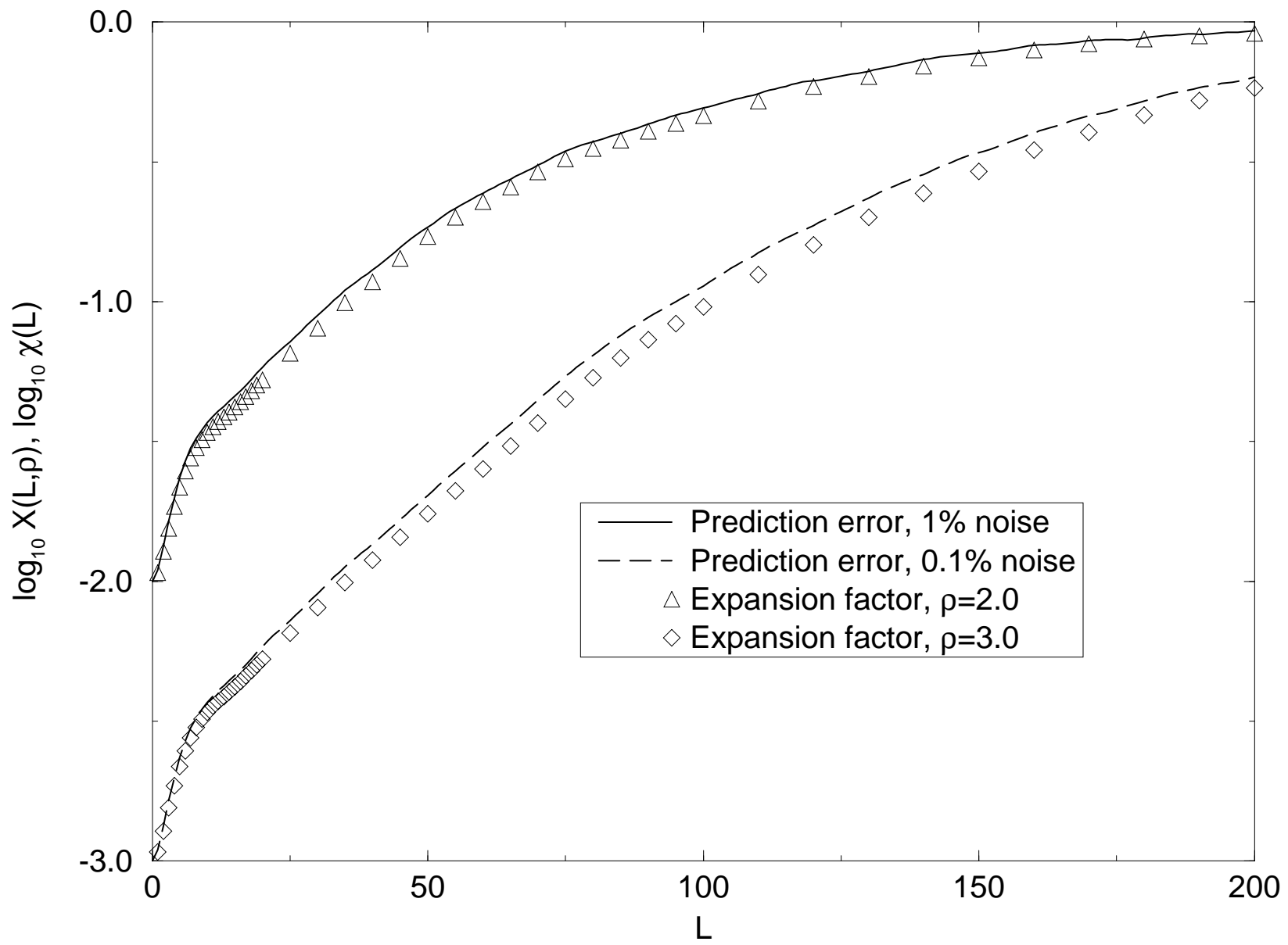
FIG. 3. $\log_{10} \chi(L)$ (solid lines) and $\log_{10} X(L, \rho)$ (symbols) using known flow equations and varying sizes of initial perturbations.

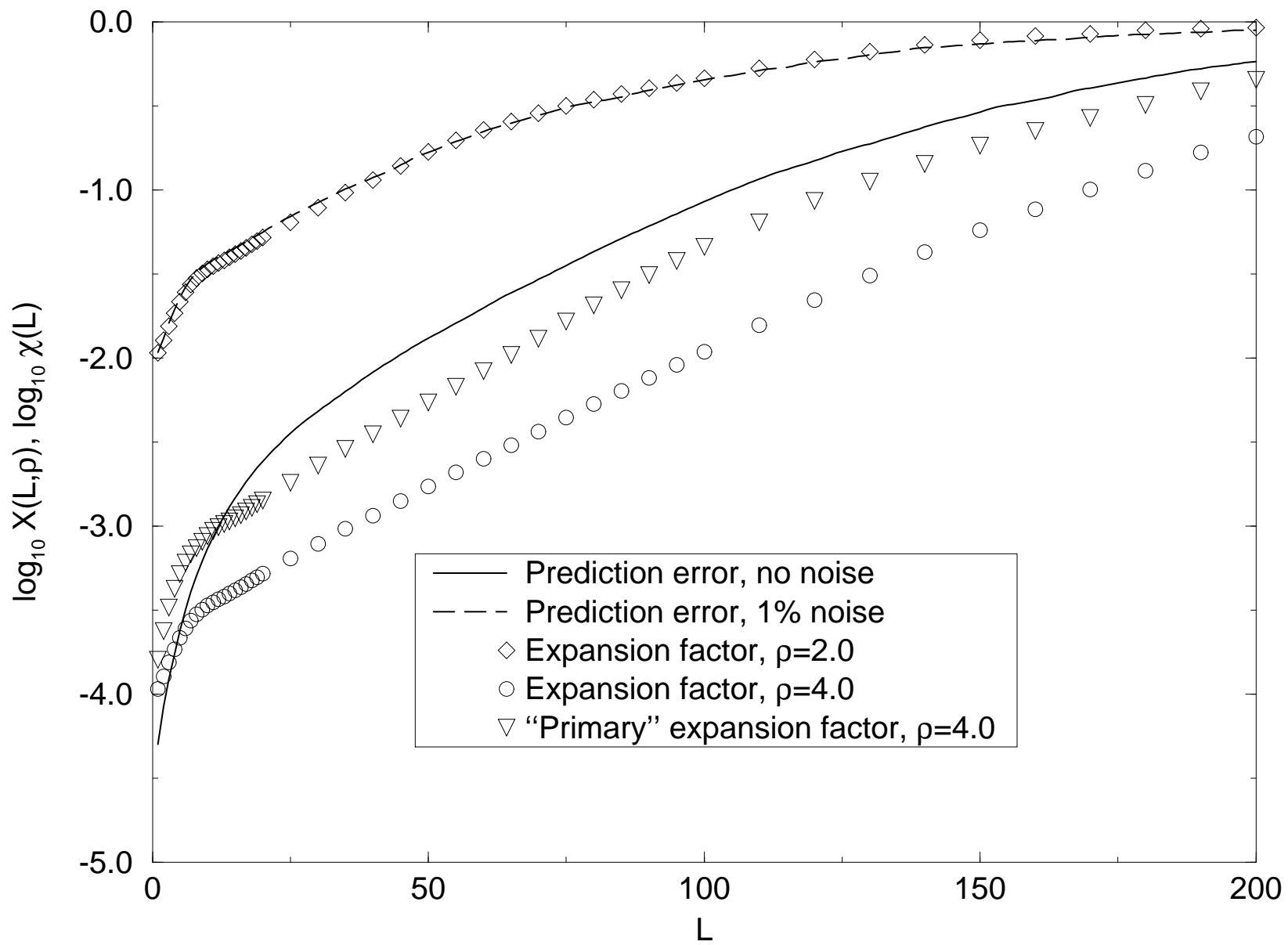
FIG. 4. $\log_{10} \chi(L)$ and $\log_{10} X(L, \rho)$ (symbols) using local quadratic prediction, with no initial perturbation (solid line), and a 1% perturbation (dashed line) before prediction.

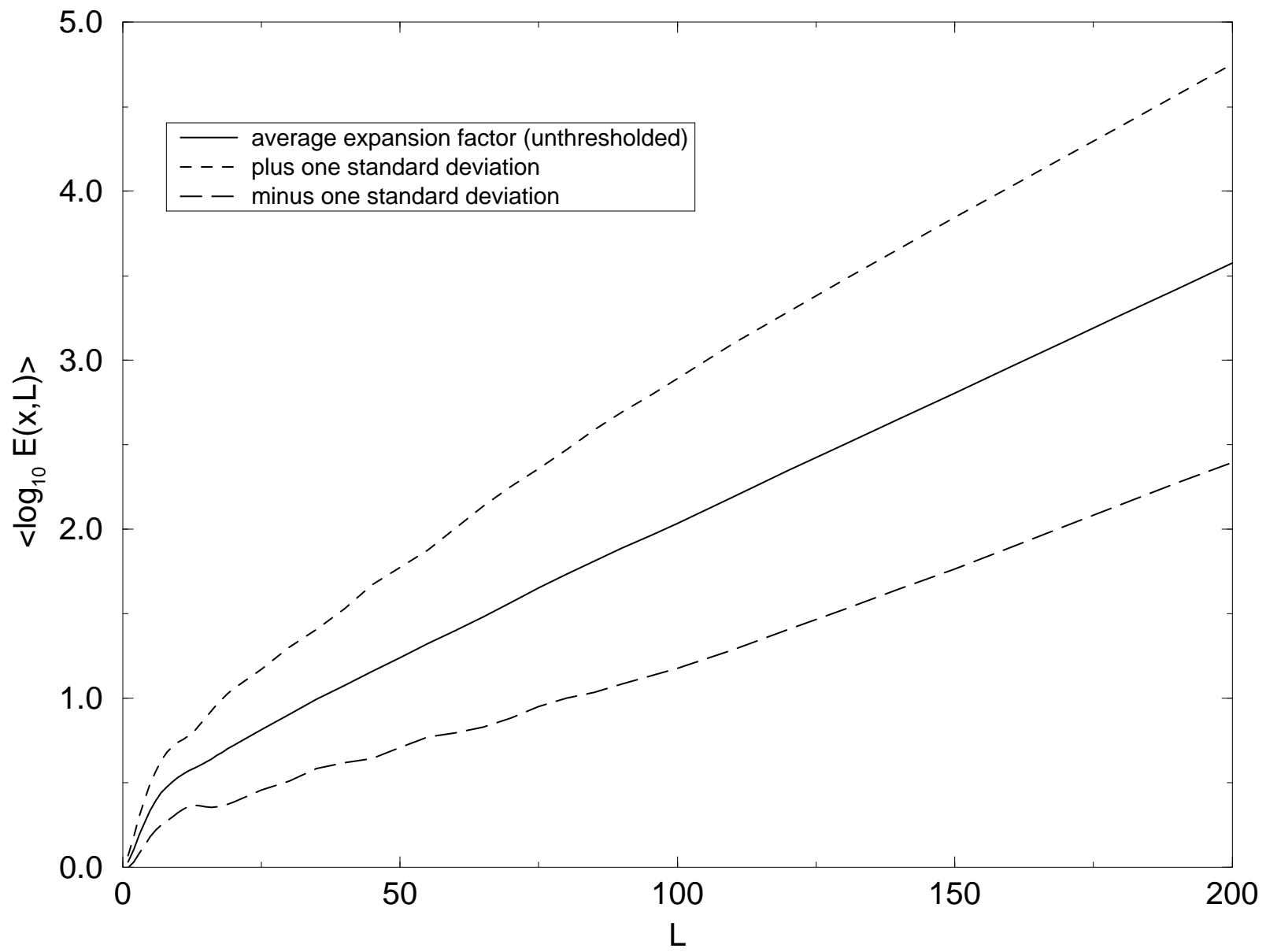
FIG. 5. Geometric mean of local expansion factors (solid line), plus one standard deviation of the distribution (dotted line) and minus one standard deviation (dashed line), for Lorenz flow.











Prediction Errors and Local Lyapunov Exponents

Matthew B. Kennel*
Institute for Nonlinear Science
and
Department of Physics

Henry D. I. Abarbanel†
Department of Physics
and
Marine Physical Laboratory
Scripps Institution of Oceanography
and
Institute for Nonlinear Science

J. J. (“Sid”) Sidorowich‡
Institute for Nonlinear Science University of California, San Diego

Mail Code 0402
La Jolla, CA 92093-0402
(March 3, 1994)

Abstract

It is frequently asserted that in a chaotic system two initially close points will separate at an exponential rate governed by the largest global Lyapunov exponent. Local Lyapunov exponents, however, are more directly relevant to predictability. The difference between the local and global Lyapunov exponents, the large variations of local exponents over an attractor, and the saturation of error growth near the size of the attractor—all result in non-exponential scalings in errors at both short and long prediction times, sometimes even obscuring evidence of exponential growth. Failure to observe exponential error scaling cannot rule out deterministic chaos as an explanation. We demonstrate a simple model that quantitatively predicts observed error scaling from the local Lyapunov exponents, for both short and surprisingly long times. We comment on the relevance to atmospheric predictability as studied in the meteorological literature.

05.45.+b,92.60.Wc

Typeset using REVTeX

Chaotic behavior in dynamical systems is intermediate between precisely predictable, regular evolution and completely unpredictable, stochastic evolution. The global Lyapunov exponents [1,2] quantify the evolution of perturbations as the system evolves for long times. A positive global Lyapunov exponent implies that errors grow to the overall size of the attractor limiting predictability to finite times.

Given observed data from a chaotic source, one can construct accurate empirical predictors [3,4,6] which allow predictions for finite times—without any knowledge of the underlying dynamics. Positive global Lyapunov exponents causes the errors in these predictions to grow exponentially rapidly, and it is conventionally assumed that the prediction error $E(t)$ will grow as

$$E(t) = E(0) \exp(\lambda_1 t). \quad (1)$$

λ_1 is the largest global Lyapunov exponent. Indeed this error growth is used as a diagnostic of deterministic chaos in the analysis of observed data [4,5].

This paper is devoted to a closer examination of this common assumption, and we will show it is often *incorrect* for times where the system is predictable. For $t \rightarrow \infty$ the largest global Lyapunov exponent λ_1 is defined in terms of a long-term average growth rate, but it does not always reflect the actual growth of prediction errors in finite time. Further for $t \rightarrow \infty$ the perturbed orbit, although eventually uncorrelated with the reference orbit, is constrained to stay on the attractor, and thus the size of a perturbation will saturate near the overall size of the attractor. Reconciling these two aspects of error growth leads to our improvement to Equation (1).

We briefly review the definition of local Lyapunov exponents. Our discrete time dynamical system is $\mathbf{y}(n+1) = \mathbf{F}(\mathbf{y}(n))$. Small perturbations $\delta\mathbf{y}(n)$ to this orbit evolve L steps forward in time according to the linearized dynamics

$$\delta\mathbf{y}(n+L) = \mathbf{DF}^L(\mathbf{y}(n)) \cdot \delta\mathbf{y}(n). \quad (2)$$

With $\mathbf{DF}_{ab}(\mathbf{y}) = \partial F_a(\mathbf{y})/\partial y_b$ the Jacobian matrix of the dynamics, we denote $\mathbf{DF}^L(\mathbf{y}(n)) = \prod_{i=0}^{L-1} \mathbf{DF}(\mathbf{y}(n+i))$. The Oseledec matrix [2],

$$\mathbf{O}(\mathbf{y}, L) = [(\mathbf{DF}^L(\mathbf{y}))^T \cdot \mathbf{DF}^L(\mathbf{y})]^{1/2L} \quad (3)$$

has eigenvalues $e^{\lambda_1(\mathbf{y},L)}, e^{\lambda_2(\mathbf{y},L)}, \dots, e^{\lambda_d(\mathbf{y},L)}$, in d -dimensions. We order the exponents as $\lambda_1 \geq \lambda_2 \geq \lambda_3 \dots \geq \lambda_d$. These **local** exponents $\lambda_a(\mathbf{y}, L)$ address the growth (or decay) over L time steps of perturbations made around some point \mathbf{y} in the state space. As $L \rightarrow \infty$ $\lambda_a(\mathbf{y}, L) \rightarrow \lambda_a$, the global exponents.

Taken over an initially isotropic distribution the initial root-mean-squared Euclidean distance of the *evolved* perturbation vectors to the origin will grow by $(\frac{1}{d} \sum_{i=1}^d \Lambda_i^2)^{1/2}$. $\Lambda_a(\mathbf{x}, L) = \exp[L\lambda_a(\mathbf{x}, L)]$. Lorenz first derived this formula in an early paper [9]. We employ the analogous quantity appropriate for a geometric mean instead of the arithmetic mean. We found this to be $\frac{1}{d} \sum_{i=1}^d \Lambda_i$ via numerical experiment, though we do not yet know of a simple, general derivation corresponding to that in reference [9]. We note that direct numerical computation of the matrix product of many Jacobians leads to ill-conditioning, and thus for practical computation we employ the algorithm of reference [8] to stably compute the local Lyapunov exponents.

The quantity $E(\mathbf{x}, L) = \frac{1}{d} \sum_{i=1}^d \Lambda_i(\mathbf{x}, L)$, which we denote the “expansion factor”, quantifies the multiplicative growth of typical predictor errors starting at \mathbf{x} , looking ahead L steps. The expansion factor is best calculated from local exponents as

$$\begin{aligned} \log E(\mathbf{x}, L) = & L\lambda_1(\mathbf{x}, L) + \log[1 + e^{L(\lambda_2(\mathbf{x},L)-\lambda_1(\mathbf{x},L))} + e^{L(\lambda_3(\mathbf{x},L)-\lambda_1(\mathbf{x},L))} + \dots \\ & + e^{L(\lambda_d(\mathbf{x},L)-\lambda_1(\mathbf{x},L))}] - \log d \end{aligned} \quad (4)$$

For increasing L , $\lambda_1(\mathbf{x}, L)$ quickly dominates the expansion factor. This also motivates Equation (1), but here $\lambda_1(\mathbf{x}, L)$, is the *finite-time* Lyapunov exponent, which does not converge very quickly to λ_1 . [7].

The other ingredient in our model for the average prediction error is a saturation cutoff. If we limit the maximal expansion factor for each initial condition to a constant R , we then compute the geometric mean (over reference points on the attractor $\mathbf{x}(i)$) of the expansion factors $E(\mathbf{x}, L)$, which is the arithmetic mean of $\log E(\mathbf{x}, L)$, hard-limited by $\rho = \log R$:

$$\log X(L, \rho) = \frac{1}{N} \sum_{i=1}^N \min[\log E(\mathbf{x}(i), L), \rho] - \rho. \quad (5)$$

The saturation cutoff models the fact that finite-sized perturbations and prediction errors cannot grow indefinitely. We estimate R is the ratio of the geometric mean of $|\mathbf{x}(i) - \mathbf{x}(j)|$ over uncorrelated pairs of attractor points to the geometric mean of the initial perturbation

magnitude. Larger R corresponds to better predictability. Note that we are averaging individually thresholded expansion factors—not thresholding an average expansion factor. Before the saturation sets in $\log X(L) \approx L\bar{\lambda}(L)$, with $\bar{\lambda}(L)$ the average finite-time Lyapunov exponent [7,8].

We now compare (1) the growth of errors actually incurred by making repeated predictions and (2) the growth rate implied by the thresholded expansion factors, Equation (5). This suggests that prediction errors grow as do the separation of initially close trajectories. This means we are considering the errors in prediction that arise from inherent dynamical instability and not inaccuracies as a result of specific features of the prediction scheme.

Our measure of average prediction error is the geometric mean over initial conditions of an L -step iterated predictor, a composition of L one-step predictors. The error is normalized by the geometric mean distance between all time-decorrelated pairs of points on the attractor, so that the absence of predictability corresponds to zero logarithmic error. With $\mathbf{G}(\bullet)$ the one-step predictor, the normalized prediction error L steps ahead is

$$\log \chi(L) = \frac{1}{N} \sum_{i=1}^N \log |\mathbf{G}^L(\mathbf{x}(i)) - \mathbf{x}(i+L)| - \frac{1}{N^2} \sum_{i,j=1}^N \log |\mathbf{x}(i) - \mathbf{x}(j)|. \quad (6)$$

As for $\log X(L, \rho) \lim_{L \rightarrow \infty} \log \chi(L) = 0$. The iterated prediction is *not* rescaled to remain close to the reference trajectory.

The main empirical result is that on chaotic attractors $\log \chi(L) = \log X(L, \rho)$ given the correct threshold ρ . We evaluate the local Lyapunov exponents, then compute the single parameter family of curves given by Equation (5) over a range of ρ . We find that once the best value of ρ is found, the resulting $\log X(L, \rho)$ quantitatively predicts the scaling of errors throughout the range of time examined. That equation (5) predicts the scaling of errors in the saturation region ($L \rightarrow \infty$) is somewhat surprising because Lyapunov exponents quantify linear expansion rates of *infinitesimal* perturbations, but in the saturation region one envisions typically large deviations. A possible explanation is that in the saturation regime average prediction error is controlled by the tail of the distribution of individual expansion factors: those initial conditions that happen to be exceptionally predictable and whose expansion factors thus remain below the threshold for especially long times. This is plausible because local Lyapunov exponents often have wide distributions [7,8].

Figure 1 shows iterated prediction errors, $\log_{10}(\chi(L))$, computed using nonlinear kernel regression [6] versus thresholded expansion factors (5) for data from the Ikeda map of the

plane to itself [10]. The data set is 20,000 real and imaginary components from the complex-valued map $z(n+1) = p + Bz(n) \exp[i\kappa - i\alpha/(1 + |z(n)|^2)]$ with parameters $p = 1.0$, $B = 0.9$, $\kappa = 0.4$, $\alpha = 6.0$. At short times, there is an obvious exponential scaling region (a line with a constant slope λ_1), as predicted by Equation (1). Starting at $L \approx 10$ the slope decreases and curves off to zero, well modeled by the thresholded expansion factor. We did not optimize ρ in any sophisticated manner, but simply stepped ρ by 0.2 and selected the best match. From a time series $\mathbf{y}(i), i = 1 \dots N$, we compute a prediction for an input vector \mathbf{x} as $\mathbf{G}(\mathbf{x}) = \left(\sum_{i=1}^N \mathbf{y}(i+1) K(\mathbf{x} - \mathbf{y}(i)) \right) / \left(\sum_{i=1}^N K(\mathbf{x} - \mathbf{y}(i)) \right)$ using a Gaussian kernel $K(\mathbf{z}) = \exp(-|\mathbf{z}|^2/\sigma^2)$ with σ set to twice the geometric mean nearest-neighbor distance of the $\mathbf{y}(i)$. This is a global prediction formula but effectively functions as a localized interpolator. The local Lyapunov exponents were calculated from this same data set [8] without the equations.

Figure 2 shows the same information for data from a three dimensional flow of Lorenz [11]. The dynamical equations are $\dot{x} = -y^2 - z^2 - a(x - F)$, $\dot{y} = xy - bxz - y + G$, $\dot{z} = bxy + xz - z$, with parameters set $a = 0.25$, $b = 4.0$, $F = 8.0$, and $G = 1.0$, sampled at intervals $\delta t = 0.2$. The attractor has a dimension of about 2.5. There is no obvious exponential scaling regime here. Given only the curve of predictor errors, one could not easily identify the Lyapunov exponent, in contrast to the previous example. The appropriately thresholded expansion factor, however, agrees with the observed scaling of prediction errors. For contrast, the graph also shows the results of choosing either too small a threshold (the circles) or too large a threshold (the triangles) for this prediction scheme and data set.

Now we examine our main result $\log \chi(L) = \log X(L, \rho)$ with a better controlled experiment. This time as our “prediction function” we use the actual dynamical equations of the Lorenz system but start the integration with an initial condition slightly perturbed from the reference point by a small uniformly distributed random vector $\eta(i)$: $\mathbf{G}^L(\mathbf{x}(i)) = \mathbf{F}^L(\mathbf{x}(i) + \eta(i))$. We directly calculate Lyapunov exponents from the known differential equations by simultaneously integrating the equations of motion and the tangent space flow. Figure 3 compares $\log \chi(L)$ with $\log X(L, \rho)$ with varying sizes of the initial perturbation. The growth of the perturbations matches the thresholded expansion factor, with the previously free parameter ρ fixed at the predicted value $\rho = \langle \log |\mathbf{x}(i) - \mathbf{x}(j)| \rangle_{i,j=1 \dots N} - \langle \log |\eta(i)| \rangle_{i=1 \dots N}$, confirming our model.

This scaling with L is generic to most low dimensional flows: a curve at low L scaling with an initially high slope, because the average largest local exponent is larger than the global

exponent [8], an exponential region (constant slope) corresponding to the global Lyapunov exponent, and a long tail curving off to zero as the finite-size threshold takes effect. The size and existence of the region of constant slope depends on the size of the initial error. If the error is large enough, there may be no region of exponential scaling as the curvature due to finite-time exponents merges with the curvature due to thresholds. Higher-dimensional data are likely to have lower initial predictability than very low-dimensional attractors, and therefore likely to show little observably exponential error scaling. Intermittent dynamics will create a wide variation in finite-time Lyapunov exponents, thus moving forward the time where saturation begins to take effect. In analyzing dynamical systems more complex than simple one or two dimensional models, requiring manifestly exponential error scaling as confirming deterministic chaos is unrealistic.

We have identified empirical prediction error with the evolution of perturbations, but the identity does not always strictly hold. Figure 4 shows the prediction errors on the same Lorenz flow [11] data using an accurate local quadratic polynomial technique [4,5]. This time, the prediction error is not satisfactorily matched by the thresholded expansion factor with any ρ , the main difference being a substantially larger slope at small L . We attribute part of this discrepancy to the assumption, used in deriving the expansion factor, that the initial perturbations are distributed uniformly in all directions. When a very accurate model, such as this one, is combined with extremely clean data, short term forecasting errors will be quite small, and the predicted trajectory will closely shadow the attractor, and thus, the unstable manifold. Therefore the initial rate of expansion will be larger than for isotropically distributed errors, being described better by a new “primary” expansion factor $L\lambda_1(\mathbf{x}, L)$ that only considers error expansion due to the single *largest* local Lyapunov exponent. This quantity increases faster at short times than the standard expansion factor, but still, it fails to precisely match the scaling of forecast error. Another discrepancy not accounted for by the expansion factor is that iterating imperfect models injects new error at every timestep, not only at the beginning. Usually exponential expansion of old error dominates new error, except at the shortest times. This effect will cause yet another increase to the slope at small times. When we add some isotropic noise to the initial condition before applying the iterated local predictor, outstanding agreement with the scaling predicted by Equation (5) is restored. We note that the divergence between straight prediction error and expansion factor is exaggerated by the particular conditions in force here: very good prediction on a

data base of very clean low-dimensional data from a smooth chaotic flow. We performed the same test on noisier experimental chaotic data and saw a smaller difference.

Is adding noise to the initial condition “cheating”? To be completely rigorous, one ought to model the distribution of prediction errors in the various directions corresponding to the local Lyapunov exponents. This is not possible without knowledge of detailed properties of the specific prediction scheme, and is obviously beyond the scope of this paper. The approximation of isotropic perturbation may often be acceptable, and can be enforced by adding artificial noise. In the context of analyzing observed data, a successful match between prediction errors (even with artificial initial perturbations) and thresholded expansion factors is a novel cross-check that affirms the validity of the modeling procedures, even if one cannot exactly quantify the error scaling for a particular prediction scheme. Accurate evaluation of Lyapunov exponents from degraded or high-dimensional data is somewhat difficult in practice, requiring good estimates of derivatives of the implied evolution function. Various reconstruction parameters, such as embedding and local manifold dimensions and time delay [8,3] may yield substantially different numerical answers for Lyapunov exponents, even if all are topologically acceptable. Further requiring a good match between expansion factors and error scaling provides a criterion for selecting among the otherwise equivalent choices. In general, we have found that prediction error scaling varies less with reconstruction parameters than Lyapunov exponents.

Figure 5 shows $\langle \log E(\mathbf{x}(i), L) \rangle$ ($\log X$ without the threshold) for the Lorenz flow. At the smallest times, the expansion factor does not in fact possess a constant slope, and only flattens out to a straight line, with slope equal to the infinite-time Lyapunov exponent after an initial transient regime. This curvature is always in the direction seen on this graph (higher slope at shorter times) and is a result of the fact that the average local Lyapunov exponent $\bar{\lambda}(L)$ approaches the global exponent from above as $L \rightarrow \infty$ [8]. This curvature explains non-exponential scaling of prediction error for early time intervals. Also shown is the mean plus and minus one standard deviation of the distribution of individual expansion factors $E(\mathbf{x}, L)$. The Figure demonstrates that the variation in local exponents as a function of initial condition causes a wide variation in expansion factor that *increases* with increasing L . The interaction of this wide distribution with the threshold results in the saturation of prediction error for longer times. The effects of the finite size of the attractor begin to manifest themselves when an appreciable number of the individual expansion factors approach the cutoff, which occurs well before the mean expansion factor does so.

Notice that the width of the distribution *increases* as $L \rightarrow \infty$; we have observed this feature in all systems we examined. An important conclusion is that even though the local Lyapunov exponent converges to a single global exponent which is *independent of initial condition*, i.e. $\lim_{L \rightarrow \infty} \lambda_1(\mathbf{x}, L) = \lambda_1$, the expansion factors of various individual initial conditions do not do so: $\lim_{L \rightarrow \infty} E(\mathbf{x}, L) \neq \bar{E}(L)$. This is because the standard deviation of the distribution of local exponents $\langle (\lambda(\mathbf{x}, L) - \bar{\lambda}(L))^2 \rangle$ typically decreases at a rate substantially slower than L^{-1} . Of course, considering global saturation, normalized error will eventually converge to unity, but this is an entirely different mechanism. The message is that considering dynamical predictability solely in view of the largest global Lyapunov exponent may be conceptually misleading as well as quantitatively inaccurate.

The temporal development of forecast error has been a prime concern of the weather forecasting community for many years, starting with work of Lorenz [9,12]. Common practice has been to hypothesize *ad hoc* relationships for the average error as a function of time; usually, in the form of a differential equation. Lorenz found [12] that increase of mean deviation between initially close initial atmospheric states could be fitted by an empirical law of the form

$$\dot{E}(t) = \alpha E(t) (1 - E(t)/E(\infty)). \quad (7)$$

A positive Lyapunov exponent motivates the first term; the inevitable saturation at maximum error, the second. Stroe and Royer [13] compared generalized parameterizations of empirical growth laws that include Lorenz's with results of large-scale atmospheric simulations and some experimental observations. The scaling of mean error at larger times, in the saturation regime, appeared to be better fit by an exponential law such as $d \log E(t)/dt = -\beta \log E(t)$, similar to results seen in our work, but a single empirical rule governing the initial growth of errors was not clearly indicated, either in this or previous studies. We explain this with the fact that the initial growth of error is governed by finite-time, rather than global, Lyapunov exponents. This results in an initial regime of non-exponential growth, second, this error growth rate depends on the coordinate system used [7]. The differing measures of phase-space distance employed by atmospheric scientists will result in different growth rates making the notion of a universal "doubling time for small errors" less useful than commonly believed. Our modeling of the error growth, which holds the mean finite-time Lyapunov exponents responsible at small error, but with their variation most important at saturation, backs up Stroe and Royer's conclusions that the infinitesimal

growth rate cannot be easily deduced from the saturation rate via fitting a single empirical formula like equation (7). One further point that we wish to make is that we have observed that using the arithmetic mean for the ensemble average of both error and expansion factors rather than the geometric results in far more “noisy” curves, and thus is it not clear whether expansion factors accurately match prediction errors with ensemble averaging in the arithmetic sense, though we suspect so. The arithmetic mean, commonly employed in meteorological literature, seems to be dominated by fluctuations in a few samples in the large error tail of the distribution. Convergence of the arithmetical ensemble average appears to require numbers of points excessively large even for this low-dimensional investigation. Choosing an arithmetical average also appears to accentuate the initial superexponential growth. Still, the qualitative behavior of error scaling seen in large-scale atmospheric simulations and experiment [13] appears compatible with our model, which we suggest as a more fundamental explanation for observed error growth. In the nonlinear dynamics literature, one example in Farmer and Sidorowich [4] demonstrated initially faster-than-exponential error scaling, but remained unexplained in that work.

With the exception of the work of Lorenz [9], the direct use of local Lyapunov exponents to quantify error growth in atmospheric dynamics is rather recent [14–16] and remains open to further development. The Lyapunov exponents have generally been previously considered only in the context of infinitesimal errors. This present work shows that accounting for a threshold apparently allows finite-time Lyapunov exponents to quantify error scaling at both small and substantially larger levels of error. Work remains concerning more realistic models, of course. Results of other low-dimensional chaotic data sets that we have examined, including experimental data, agree with the conclusions of this paper.

REFERENCES

- * E-mail: mbk@inls1.ucsd.edu
† E-mail: hdia@hamilton.ucsd.edu
‡ E-mail: sid@inls1.ucsd.edu
- [1] Eckmann, J.-P. and D. Ruelle “Ergodic Theory of Chaos and Strange Attractors” *Rev. Mod. Phys.* **57**, 617 (1985).
- [2] Oseledec, V. I., “A Multiplicative Ergodic Theorem. Lyapunov Characteristic Numbers for Dynamical Systems” *Trudy Mosk. Mat. Obsc* **19**, 197 (1968); *Moscow Math. Soc.* **19**, 197 (1968).
- [3] Abarbanel, H. D. I., R. Brown, J. (“Sid”) Sidorowich, and Lev Sh. Tsimring, “The Analysis of Observed Chaotic Data in Physical Systems”, *Reviews of Modern Physics* **65**, 1331-1392 (1993).
- [4] J. D. Farmer and J. Sidorowich, *Phys. Rev. Lett.*, **59**, 845 (1987)
- [5] J. D. Farmer and J. Sidorowich, “Exploiting Chaos to Predict the Future and Reduce Noise”. In *Evolution, Learning and Cognition*, ed. Y.C. Lee, World Scientific, Singapore (1988)
- [6] H. D. I. Abarbanel, R. Brown, and J. B. Kadtko, “Prediction in Chaotic Nonlinear Systems: Methods for Time Series with Broadband Fourier Spectra”, *Phys. Rev. A* **41**, 1782 (1990).
- [7] H. D. I. Abarbanel, R. Brown, and M. B. Kennel, “Variability of Lyapunov Exponents on a Strange Attractor”, *Journal of Nonlinear Science*, **1**, 175-199 (1991).
- [8] H. D. I. Abarbanel, R. Brown, and M. B. Kennel, “Local Lyapunov Exponents from Observed Data”, *Journal of Nonlinear Science* **2**, 343-365 (1992).
- [9] E. N. Lorenz, *Tellus* **17**, 321-333 (1965)
- [10] K. Ikeda, *Opt. Commun.* **30**, 257 (1979).
- [11] E. N. Lorenz, *Tellus* **36A**, 98-110 (1984).
- [12] E. N. Lorenz, *J. Atmos. Sci.* **26** 636-646 (1969)
- [13] R. Stroe, J.F. Royer, *Ann. Geophysicae* **11**, 296-316 (1993)
- [14] B.F. Farrell *J. Atmos. Sci.* **47** 2409-2416 (1990)
- [15] J.M. Nese, J.A. Dutton *J. Climate* **6** 185-203 (1993)
- [16] S. Yoden, M. Nomura *J. Atmos. Sci* **50** 1531-1543 (1993)

FIGURES

FIG. 1. $\log_{10} \chi(L)$ (solid line) and $\log_{10} X(L, \rho)$ (circles) for the Ikeda map. $\rho = 2.4$ gives a good fit.

FIG. 2. $\log_{10} \chi(L)$ (solid line) and $\log_{10} X(L, \rho)$ for data from the Lorenz flow, with $\rho = 1.2$ (triangles), $\rho = 1.6$ (circles), and $\rho = 2.0$ (diamonds).

FIG. 3. $\log_{10} \chi(L)$ (solid lines) and $\log_{10} X(L, \rho)$ (symbols) using known flow equations and varying sizes of initial perturbations.

FIG. 4. $\log_{10} \chi(L)$ and $\log_{10} X(L, \rho)$ (symbols) using local quadratic prediction, with no initial perturbation (solid line), and a 1% perturbation (dashed line) before prediction.

FIG. 5. Geometric mean of local expansion factors (solid line), plus one standard deviation of the distribution (dotted line) and minus one standard deviation (dashed line), for Lorenz flow.